Linear Subband Predictive Filters for Wideband Signals

YAN WU
Department of Mathematical Sciences
Georgia Southern University
Statesboro, GA 30460
UNITED STATES OF AMERICA

Abstract: - In this paper we present the design of multiband linear subband prediction (LSP) filters for wideband signals. A wideband signal is divided into narrowband subband signals via an array of lowpass/bandpass filters. A linear prediction filter is designed for each subband channel, which has its own designated frequency interval. The filter coefficients are fixed throughout the coding process. A closed form bound on the error of prediction shows that the LSP approach is accurate for wideband signals, which is further supported by simulations.

Key-Words: - Bandlimited, finite impulse response, subband, predictive filter, wideband, Toeplitz.

1 Introduction

Linear prediction of wideband signals is a challenging task. This is true no matter if it is viewed from the time domain or the frequency domain. In the time domain, a wide-band signal exhibits drastic changes within a short period of time. The frame size has to be downscaled to accommodate the random type behavior of the signal, which leads to a significant amount of increase in computation. Meanwhile, because of the wide range of the spectrum, it requires higher order (all-pole) models for the spectral matching if prediction is done in the frequency domain. Traditionally, linear prediction is viewed as an autocorrelation-domain analysis, which can be approached from either the time or the frequency domain [3]. The most common linear prediction filters are all-pole models built on an autocorrelation method usually associated with windowing, a covariance method, or their variant [1], [4], [5], [8]. A common feature of those methods is that the filter coefficients are obtained from solving the autocorrelation normal equations, known as the Yule-Walker equations. Those equations are constructed with the autocorrelation function values from the samples of a signal. Therefore, the filter coefficients depend on signal samples. They have to be recalculated whenever the window shifts to a new position. Mugler and Wu proposed linear prediction models for lowpass and bandpass signals in [6], [7]. The filter coefficients are independent of the samples of the input signal. Those linear prediction models are used here in the design of the so-called linear subband prediction (LSP) filters.

We adopt the idea of subband coding [2] commonly used in digital speech coding in the design of LSP filters. However, there is no down-sampling or up-sampling in the LSP filtering. The LSP filter design follows an analysis-to-synthesis structure. A wideband signal is first divided into subband signals via an array of lowpass/bandpass filters. Then, a linear prediction filter is designed for each subband signal, see Fig. 1. The filter coefficients only depend on the frequency interval of the corresponding subband. The final synthesized prediction is obtained as a sum of the subband predictions. Detailed structure of LSP filters is discussed in section 2. The motivation of this work is due to the fact that the accuracy of linear prediction of lowpass and bandpass signals improves as the bandwidth of the signal decreases [6], [7]. A closed form bound on the error of prediction is presented in section 3 followed by numerical results given in section 4. The small upper bound indicates that the LSP method is accurate for bandlimited signals. It is particularly effective and accurate for the extrapolation of wideband signals.

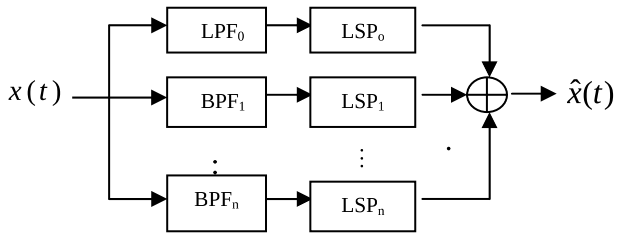

Fig.1. Structure of linear subband prediction filter design

2 Derivation of LSP Filters

In this section, we construct a series of linear subband prediction filters by first utilizing an array of filter banks to divide a bandlimited signal into lowpass and bandpass signals with narrow bandwidths. The frequency range for the baseband, i.e. $[0, f_0]$, and each successive passband are defined, for example, the i_{th} subband is restricted to $[f_{i-1}, f_i]$. We then derive a predictive formula for each subband prediction filter. The prediction coefficients only depend on the time-bandwidth product of the channel, and are independent of the signal in terms of its magnitude. They are fixed throughout the process of prediction. A schematic diagram for the linear subband prediction filter design is illustrated in Fig.1. To set the stage, let $x^{(0)}(t)$ and $x^{(i)}(t)|_{i=1,2,\dots,n}$ be the baseband and passband components of the original signal $x(t)$, which is given as follows:

$$x(t) = x^{(0)}(t) + \sum_{i=1}^{n} x^{(i)}(t). \qquad (1)$$

The Fourier transforms of the subband signals are given as follows:

$$x^{(0)}(t) = \int_{-f_0}^{f_0} X(f) e^{j2\pi ft} df \qquad (2)$$

and

$$x^{(i)}(t) = \int_{I_{[f_{i-1}, f_i]}} X(f) e^{j2\pi ft} df \qquad (3)$$

where $X(f)$ is the Fourier transform of $x(t)$ and the interval $I_{[f_{i-1}, f_i]} = [-f_i, -f_{i-1}] \cup [f_{i-1}, f_i]$.

Now, we proceed to the design of subband predictive formula based on past samples from each subband signal given by

$$\hat{x}(t) = \underbrace{b^{(0)} * \bar{x}^{(0)}}_{\text{baseband}} + \underbrace{\sum_{i=1}^{n} b^{(i)} * \bar{x}^{(i)}}_{\text{passbands}}. \qquad (4)$$

The symbol * represents convolution, and the two convolutions in (4) are defined as

$$\hat{x}^{(0)} \overset{\Delta}{=} b^{(0)} * \bar{x}^{(0)} = \sum_{k=1}^{N_0} b_k^{(0)} x^{(0)}(t - kT) \quad (5)$$

and

$$\hat{x}^{(i)} \overset{\Delta}{=} b^{(i)} * \bar{x}^{(i)} = \sum_{k=1}^{N_i} b_k^{(i)} x^{(i)}(t - kT), i = 1,2,\dots,n. \quad (6)$$

We assume that the signal is uniformly sampled with sampling interval *T*. Meanwhile, the vectors in (5) and (6), $b^{(0)}$ and $b^{(i)}, i = 1,2,\dots,n$, consist of the predictive filter coefficients for the baseband signal $x^{(0)}$ and the i_{th} passband signal $x^{(i)}$ respectively. The order of the i_{th} subband predictive filter is given by N_i. It is chosen based on the scale of the time-bandwidth product [6], [7], i.e. $2Tf_0$ for baseband and $T(f_i - f_{i-1})$ for passband, of the corresponding subband channel. Generally speaking, the order of a subband predictive filter is less than ten if the time-bandwidth product of the subband is less than 0.5.

The coefficients for the predictive filters are derived from minimizing the net error of prediction, i.e.

$$\varepsilon = |x(t) - \hat{x}(t)|.$$

By using the triangle inequality, the problem of minimizing the error of prediction ε can be decoupled into a series of minimization problems over the individual subband channels, i.e.

$$\varepsilon = \left| \sum_{m=0}^{n} x^{(m)} - \sum_{l=0}^{n} \hat{x}^{(l)} \right| \le \sum_{m=0}^{n} \left| x^{(m)} - \hat{x}^{(m)} \right|.$$

This allows us to incorporate narrow subbands into the minimization process. It turns out in the frequency domain that the error minimization is transformed into minimizing the Fourier integral of each subband filter over its entire bandwidth. By applying the well-known Cauchy-Schwarz inequality to $\left|x^{(m)} - \hat{x}^{(m)}\right|, m = 0,1,\dots,n,$ one obtains

$$\varepsilon \le \left\|x^{(0)}\right\| \sqrt{\int_{-f_0}^{f_0} \left|1 - d^{(0)}(fT)\right|^2 df} + \sum_{i=1}^{n} \left\|x^{(i)}\right\| \sqrt{\int_{I_{[f_{i-1}, f_i]}} \left|1 - d^{(i)}(fT)\right|^2 df} \overset{\Delta}{=} \left\|x^{(0)}\right\| \varepsilon_0 + \sum_{i=1}^{n} \left\|x^{(i)}\right\| \varepsilon_i \quad (7)$$

where $\left\|x^{(i)}\right\| = \sqrt{\int_{-\infty}^{\infty} \left|x^{(i)}(t)\right|^2 dt}, i = 0,1,\dots,n,$ which represents the energy of the subband signals. Meanwhile,

$$d^{(i)}(fT) = \sum_{k=1}^{N_i} b_k^{(i)} e^{-j2\pi kfT}, i = 0,1,\dots,n. \qquad (8)$$

The filter coefficients, $b_k^{(i)}$, are obtained from minimizing the error integrals ε_0 and ε_i from (7) respectively, which is a standard least-squares problem. The filter coefficients for the baseband, $b_k^{(0)}$, satisfy the following Toeplitz system:

$$H^{(0)}b^{(0)} = h^{(0)} \text{ (baseband)} \qquad (9)$$

where

$$H^{(0)} = \begin{bmatrix} s_0(0) & s_0(T) & \ldots & s_0((N_0-1)T) \\ s_0(T) & s_0(0) & \ldots & s_0((N_0-2)T) \\ \ldots & & \ldots & \\ s_0((N_0-1)T) & s_0((N_0-2)T) & \ldots & s_0(0) \end{bmatrix}_{N_0 \times N_0}$$

and

$$b^{(0)} = \begin{bmatrix} b_1^{(0)} & b_2^{(0)} & \ldots & b_{N_0}^{(0)} \end{bmatrix}^{\mathrm{T}},$$

$$h^{(0)} = \begin{bmatrix} s_0(T) & s_0(2T) & \ldots & s_0(N_0T) \end{bmatrix}^{\mathrm{T}}$$

where $s_0(t) = \mathrm{sinc}(\tau_0 t)$, in which $\mathrm{sinc}(t) = \frac{\sin \pi t}{\pi t}$ and $\tau_0 = 2f_0$ (f_0 is the bandwidth of the baseband). The Toeplitz system needed for the computation of the filter coefficients for each passband, $b_k^{(i)}$, is given by

$$H^{(i)}b^{(i)} = h^{(i)}, i = 1,2,\ldots,n \text{ (passband)} \qquad (10)$$

where

$$H^{(i)} = \begin{bmatrix} s_1(0) & s_1(T) & \ldots & s_1((N_i-1)T) \\ s_1(T) & s_1(0) & \ldots & s_1((N_i-2)T) \\ \ldots & & \ldots & \\ s_1((N_i-1)T) & s_1((N_i-2)T) & \ldots & s_1(0) \end{bmatrix}_{N_i \times N_i}$$

and

$b^{(i)} = \begin{bmatrix} b_1^{(i)} & b_2^{(i)} & \ldots & b_{N_i}^{(i)} \end{bmatrix}^{\mathrm{T}}$, $h^{(i)} = \begin{bmatrix} s_1(T) & s_1(2T) & \ldots & s_1(N_iT) \end{bmatrix}^{\mathrm{T}}$,

where $s_1(t) = \cos(2\pi f_{ic} t)\mathrm{sinc}(\tau_i t)$ with $\tau_i = f_i - f_{i-1}$, bandwidth of the i_{th} passband, and $f_{ic} = \frac{f_{i-1} + f_i}{2}$, center frequency of the i_{th} passband.

The symmetric Toeplitz systems (9) and (10) are ill-conditioned for small time-bandwidth product *TW* of the subband, where *T* is the sampling interval and *W* is the bandwidth of the subband. Therefore, we use Levinson-Durbin's recursive approach, which is well known for solving ill-conditioned Toeplitz matrix equations, to solve the N_i-dimensional Toeplitz systems (9) and (10). Once the filter coefficients are obtained from (9) and (10), they are incorporated back into (4), where the future value of a subband signal is predicted from each subband channel, and then the final synthesized prediction, $\hat{x}(t)$, is obtained by adding all the predicted values together, see Fig. 1.

An important feature of the subband predictive formula (4) is readily seen from the derivation that the filter coefficients only depend on the sampling interval and the frequency bounds for each subband, and they are independent of the sample values of the specific signal $x(t)$. Therefore, the same prediction formula (4) is applicable to two different signals as long as they share the same frequency interval even if the spectra over the frequency interval could be dramatically different between the two signals.

3 Performance Analysis

The magnitude for the error of prediction of the LSP method is not readily seen from (7) since there is no closed form expression for the minimized error integrals in (7). Nonetheless, the prediction coefficients, $b^{(i)}, i = 0,1,\ldots,n$, should yield the least upper bound on the error of prediction, ε, under the Cauchy-Schwarz inequality. In order to perceive the size of the error, which would further shed light on the accuracy of the proposed predictive method, we derive an upper bound on the error, which has a closed form expression.

The error integrals, $\varepsilon_i, i = 0,1,\ldots,n$, in (7) can be written into a quadratic form as follows

$$\varepsilon_i = \sqrt{\int_{I_{[f_{i-1}, f_i]}} \left|1 - d^{(i)}(fT)\right|^2 df} = \sqrt{v^{(i)^{\mathrm{T}}} A^{(i)} v^{(i)}} \qquad (11)$$

where $v^{(i)} = \begin{bmatrix} 1 & -b_1^{(i)} & -b_2^{(i)} & \ldots & -b_{N_i}^{(i)} \end{bmatrix}^{\mathrm{T}}$, and

$$A^{(i)} = \begin{bmatrix} 1 & h^{(i)^{\mathrm{T}}} \\ h^{(i)} & H^{(i)} \end{bmatrix} \qquad (12)$$

where $h^{(i)}$ and $H^{(i)}$ are defined in (9) and (10) respectively. We are able to find a special $v^{(i)}$ so that $\sqrt{v^{(i)^{\mathrm{T}}} A^{(i)} v^{(i)}}$ can be expressed in terms of the smallest eigenvalue of $A^{(i)}$. Let λ_i be the smallest eigenvalue of $A^{(i)}$ and the corresponding eigenvector with unit length, $u^{(i)} = \begin{bmatrix} u_0^{(i)} & u_1^{(i)} & \ldots & u_{N_i}^{(i)} \end{bmatrix}^{\mathrm{T}}$, then

$$\sqrt{u^{(i)^{\mathrm{T}}} A^{(i)} u^{(i)}} = \sqrt{\lambda_i}. \qquad (13)$$

Without loss of generality, we assume that $u_0^{(i)}$ is positive. The eigenvector $u^{(i)}$ can be scaled with $u_0^{(i)}$ so that eqn. (13) can be written as

$$\sqrt{\left(\frac{u^{(i)^{\mathrm{T}}}}{u_0^{(i)}}\right) A^{(i)} \left(\frac{u^{(i)}}{u_0^{(i)}}\right)} = \frac{\sqrt{\lambda_i}}{u_0^{(i)}}. \qquad (14)$$

Therefore, let $b_k^{(i)} = -\frac{u_k^{(i)}}{u_0^{(i)}}, k = 1,2,\ldots,N_i$, then a closed form expression for ε_i is obtained as follows

$$\varepsilon_i = \frac{\sqrt{\lambda_i}}{u_0^{(i)}} \tag{15}$$

where λ_i is the smallest eigenvalue of the augmented matrix $A^{(i)}$ in (12). Hence, the size of the error integral ε_i largely depends on the magnitude of the smallest eigenvalue λ_i. Finally, a closed form for the upper bound of the error of prediction is given by

$$\varepsilon \le \left\| x^{(0)} \right\| \cdot \frac{\sqrt{\lambda_0}}{u_0^{(0)}} + \sum_{i=1}^{n} \left\| x^{(i)} \right\| \cdot \frac{\sqrt{\lambda_i}}{u_0^{(i)}} \tag{16}$$

where λ_0 is the smallest eigenvalue of the augmented matrix (12) obtained from $H^{(0)}$ given by (9) and $\lambda_i, i = 1,2,...,n$, is the smallest eigenvalue of the augmented matrix (12) obtained from $H^{(i)}$ given by (10). It is important to identify that the augmented matrix (12) is a symmetric Toeplitz matrix and it is positive definite [10].

As noted earlier, the Toeplitz matrices such as the ones in (9), (10), and (12) are ill-conditioned. Recall that a matrix is ill-conditioned if its condition number is large. Since our Toeplitz matrices are symmetric (and positive definite), its condition number has the following expression

$$\text{cond}\,(A^{(i)}) = \frac{\lambda_{\max}^{(i)}}{\lambda_{\min}^{(i)}} \tag{17}$$

where $\lambda_{\min}^{(i)}$ and $\lambda_{\max}^{(i)}$ are the extreme eigenvalues of $A^{(i)}$ respectively. Therefore, a large condition number of $A^{(i)}$ implies a small value of $\lambda_{\min}^{(i)}$. This is true because $\lambda_{\max}^{(i)}$ cannot be too large due to the fact that $\lambda_{\max}^{(i)}$ is less than the trace of $A^{(i)}$, which equals $N_i + 1$. Numerical calculation of the eigenvalues of $A^{(i)}$ further confirms that the eigenvalue $\lambda_{\min}^{(i)}$ is small if the bandwidth parameter is small, see Fig. 2a. As a result, the upper bound on the error of prediction (16) is small as long as the bandwidth for each subband is small, which implies high accuracy of prediction.

It is generally true that the more samples (more redundancy of information) used in a predictive formula the better accuracy of the prediction. It is certainly true for the LSP filters. The number of samples used in a subband predictive formula, (5) and (6) (N_i-tap prediction), is related to the dimension of the matrix (12) in such a way that, if the number of samples is N_i, the dimension of the augmented matrix (12) is $(N_i + 1) \times (N_i + 1)$. It is shown in Fig. 2b that the smallest eigenvalue of the matrix monotonically decreases and approach zero as the dimension of the matrix increases, which, from (16), implies higher accuracy of prediction with more samples.

The above analysis leads to two different approaches for implementing the subband predictive method to achieve the same accuracy of prediction. The first approach is to use less filter banks but more samples from each subband to carry out the prediction (use high-order LSP filters); the second one is to use more filter banks, which allows us to adopt less samples from each subband (use low-order LSP filters).

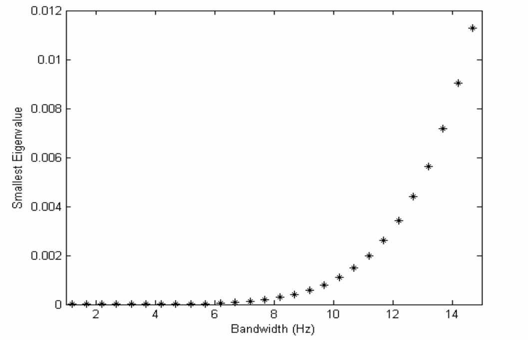

(a)

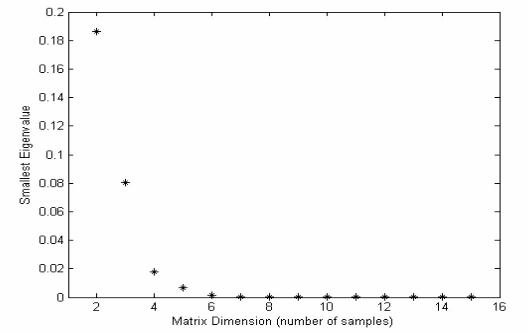

(b)

Fig.2. Smallest eigenvalue of the augmented matrix (12) vs. (a) the bandwidth parameter (b) dimension of the matrix

4 Numerical Simulation

To demonstrate the performance of the LSP filters, we apply these filters as well as linear predictive method-based (LPM) filters to a set of speech data. The LPM filters are well-known predictive filters in digital signal processing [9]. The LPM filter coefficients are signal-dependent in such a way that they are recalculated and updated on-line whenever a new frame of samples is fed through the prediction filter [9]. In contrast, the design of LSP filters is done offline, the filter coefficients are fixed throughout the process of prediction. Therefore, the LSP filter design is much more efficient than that of LPM-based filter design.

The speech signal in our numerical test is sampled at 8 kHz, and it is already bandlimited to 3.4 kHz. For the examples presented in this paper, we used DFT-based ideal lowpass/bandpass filters to divide the speech signal into subband signals. Once the cutoff frequencies are set for each subband, they are used to compute the LSP filter coefficients via (9) and (10) for the corresponding subband channel and the filter coefficients stay invariant during the process of prediction. Meanwhile, the LPM filters are also set up for the comparison. The coefficients of the LPM filters are recalculated and updated once every 80 samples.

In the first case study, we test the filters over a four-band and a six-band setting respectively. The results are summarized in Table 1. The results shown are point-wise relative error from each step of prediction. The simulation runs over 3000 samples, which are within the voiced segment of the speech data. The first two columns of Table 1 list the largest error and the smallest error out of the 3000 predictions respectively. We also record the number of predictions, of which the error satisfies the specified criterion (less than 10^{-3}). This result is shown in the third column. The upper bound for the error of prediction for LSP is computed from (16), which is listed in the fourth column of Table 1. The numerical bound would indicate the accuracy of prediction for the LSP filters.
The results listed in Table 1(a) are obtained based on the setting that the signal is first lowpassed/bandpassed to four subbands with 0.8 kHz, 0.9 kHz, 0.9 kHz, and 0.8 kHz as the bandwidths of the respective subband signals. The LSP filters include an eight-tap prediction filter for the baseband channel and a twelve-tap prediction filter for each passband channel. On the other hand, we give some leeway to the LPM filters by allowing a twelve-tap prediction filter for each subband channel. We then use a six-band setting, Table 1(b), with the following designated bandwidths: 0.406 kHz, 0.406 kHz, 0.497 kHz, 0.701 kHz, 0.698 kHz, and 0.692 kHz, to compare the performance between the two prediction filters. Under these settings, the LSP filters consist of a six-tap baseband prediction filter and a fifteen-tap prediction filter for each passband, while the LPM filters consists of a twenty-tap prediction filter for each subband. The reason we use a lower order LSP filter for the baseband channel is that the bandwidth (0.8 kHz in (a) and 0.406 kHz in (b)) is so small that the time-bandwidth product is only 0.2 in (a) and 0.1015 in (b). Therefore, to maintain the accuracy of prediction, it is sufficient to adopt a smaller number of samples to carry out the prediction. The results show that the LSP filter out-performs the LPM filter in all the measurable categories. For the last category, the LPM method does not have a uniform bound on error to compare with that of the LSP method. We did many other experiments with different segments of the speech data and different settings. The results showed that LSP filter design is consistently better than the LPM design in terms of accuracy.

Table 1. Comparison of accuracy between LSP and LPM filters: (a) a four-band setting (b) a six-band setting

	max error	min error	# of errors<1e-3	upper bound
LSP	8.7116e - 2	5.0901e - 7	2612 (out of 3000)	0.9305
LPM	4.2659e+2	1.1380e - 4	186 (out of 3000)	N/A

(a)

	max error	min error	# of errors<1e-3	upper bound
LSP	6.3625e - 3	7.3275e - 9	2941 (out of 3000)	0.1107
LPM	1.1315e+2	5.7605e - 6	417 (out of 3000)	N/A

(b)

5 Conclusion

The LSP filter design has an analysis-to-synthesis structure. The filter coefficients are determined by minimizing a series of spectral-domain error integrals, and they are fixed throughout the process of prediction. This special feature is in contrast to most prediction filters, in which the filter coefficients have to be recalculated periodically. We present a closed form upper bound on the error of prediction. The small upper bound implies highly accurate predictions, which is also verified by numerical experiments.

Future work includes the performance evaluation of LSP filters against noise (robustness) and aliasing effect, application of this method in speech processing, such as pitch detection and data compression.

References:

[1] P. L. Combettes and H. J. Trussell, Stability of the linear prediction filter: a set theoretic approach, *Proc. ICASSP*, 1988, pp. 2288-2291.
[2] B. Francis and S. Dasgupta, Signal compression by subband coding, *Automatica*, vol. 35, pp. 1895-1908, May 1999.

[3] J. Makhoul, Linear Prediction: A Tutorial Review, *Proc. of the IEEE*, vol. 63, no. 4, pp. 561-580, Apr. 1979.

[4] J. Makhoul, Spectral Linear Prediction: Properties and Applications, *IEEE Trans. Acoustics, Speech, and Signal Processing*, vol. ASSP-23, no. 3, pp. 283-296, Jun. 1975.

[5] J. Makhoul, Stable and Efficient Lattice Methods for Linear Prediction, *IEEE Trans. Acoustics, Speech, and Signal Processing*, vol. ASSP-25, no. 5, pp. 423-428, Oct. 1977.

[6] D. H. Mugler, Y. Wu, and Splettstößer, Nyquist Rates and the Linear Prediction of Band-limited Signals Based on Signal and Derivative Samples, *Proc. SampTA*, 1997, pp. 321-326.

[7] D. H. Mugler, Y. Wu, and S. Clary, Linear prediction for bandpass signals based on nonuniform past samples, *Proc. ICASSP*, 2000, pp. 3854-3857.

[8] R. P. Ramachandran and P. Kabal, Pitch Prediction Filters in Speech Coding, *IEEE Trans. Acoustics, Speech, and Signal Processing*, vol. ASSP-37, no. 4, 1989, pp. 467-478,

[9] B. Sklar, *Digital Communications: Fundamentals and Applications*, Englewood Cliffs, NJ: Prentice Hall, 1988, pp. 630-653.

[10] Y. Wu, On the positiveness of a functional symmetric matrix used in digital filter design, *Journal of Circuits, Systems, and Computers*, vol. 13, no. 5, 2004, pp. 1105-1110,